THE JOURNAL OF PHYSICAL CHEMISTRY C

ACS AUTHORCHOICE

pubs.acs.org/JPCC Article

Strong Chemical Interaction and Self-Demetalation of Zinc-Phthalocyanine on Al(100)

Daniele Paoloni, Gianluca Di Filippo, Dean Cvetko, Gregor Kladnik, Alberto Morgante, and Alessandro Ruocco*

Cite This: J. Phys. Chem. C 2020, 124, 22550−22558

Read Online

ACCESS | Metrics & More | Article Recommendations

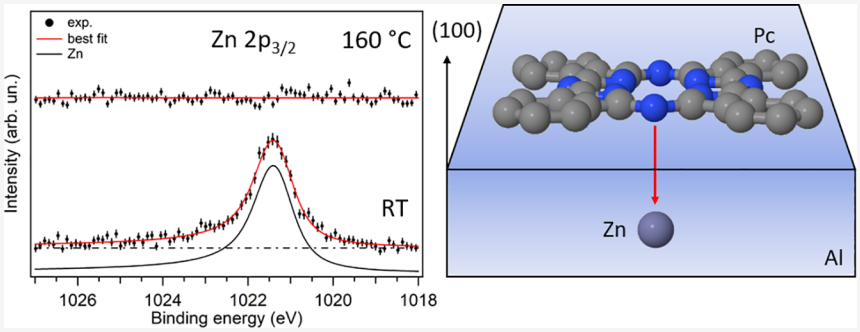

ABSTRACT: We investigate the early stages of the growth of zinc-phthalocyanine on Al(100) using X-ray photoemission spectroscopy (XPS) and low-energy electron diffraction (LEED). Diffraction patterns show a (5 × 5) reconstruction, characteristic of flat-lying molecules forming a long-range-ordered structure with a square unit cell. The degree of ordering (i.e., the average domain size) is increased when the substrate is kept above 100 °C during the deposition. At low coverage (≤1 ML), a sizeable charge transfer from the substrate to the molecules is observed, indicating a strong interaction at the organic−inorganic interface. As a consequence of charge filling of ZnPc LUMO, a self-demetalation of the molecule occurs while the structure of the ligand remains mostly unaffected.

INTRODUCTION

Phthalocyanines (Pcs) are planar organometallic complexes with extended π-conjugation. They are well known for their thermal and chemical stabilities[1] while its electronic structure makes them largely used in optoelectronics,[2] fabrications of sensors[3−5] and organic semiconductor devices,[6] and as optical absorbers in organic solar cells.[7,8] Many of these applications are related to the energy gap between the highest occupied molecular orbital (HOMO) and the lowest unoccupied molecular orbital (LUMO) that falls in the visible range.[9]

One of the most important peculiarities of this molecule is the possibility to synthesize them with different atoms in the center of the molecule ranging from the so-called free Pc with two hydrogen atoms in the center (H_2Pc) to different metal (MPc) or nonmetal atoms.[10] Different atoms in the center of the molecule give rise to different symmetries and electronic structures of the whole molecule. For instance, in the case of transition metal Pc, the b_{1g} molecular state derived from the 3d atomic level is known to vary its energy and occupancy as a function of the specific atom.[9] Other original properties are related to the central metal atom, for instance, the spin state of FePc molecules on Au(111) can be tuned by the adsorption of different ligands on Fe ions.[11] Further, the reversible vertical movement of the central metal ion through the molecular plane of a Pc molecule is a prototype of single-molecule switch.[12] To exploit the interface properties, Pcs are normally grown on different substrates (either metallic or nonmetallic). When Pc molecules are interacting with a specific substrate, the central metal atom can play a peculiar role that is important to be investigated. In fact, the surface can induce variation of the overall electronic structure of the molecule[13] but it can also induce modifications involving mainly the central atom. In the latter category, we find the metalation of the free-Pc[14,15] where the two H atoms are replaced by a metal atom. Pc metalation has been obtained by depositing iron atoms on the H_2Pc film grown on Pb(111)[14] or Ag(111)[15] with the final result of the development of FePc. The metalation on a surface can be aided by the scanning tunneling

Received: July 30, 2020
Revised: September 11, 2020
Published: September 16, 2020

https://dx.doi.org/10.1021/acs.jpcc.0c06980
J. Phys. Chem. C 2020, 124, 22550−22558

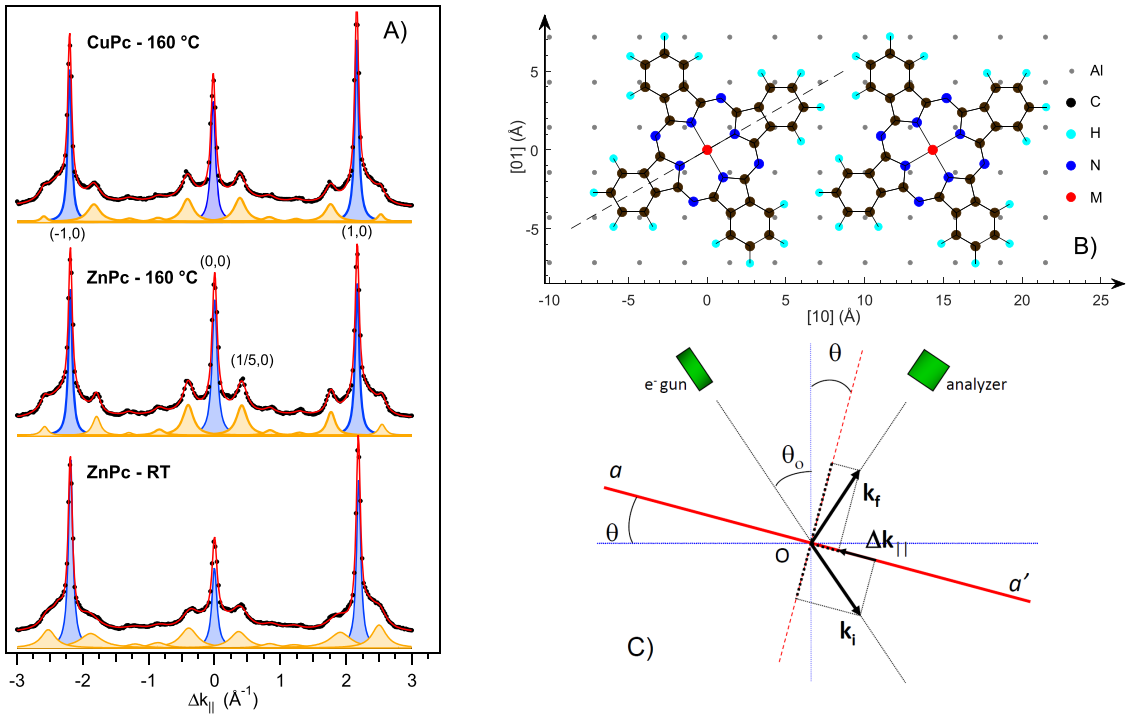

Figure 1. (A) Electron diffraction patterns along the $\overline{\Gamma}\overline{X}$ high-symmetry direction of 1 Å ZnPc/Al(100) grown at different T_s's and, for comparison, the diffraction pattern of CuPc on the same substrate and same thickness grown at T_s = 160 °C. The blue-shaded peaks represent the diffraction peaks of the clean aluminum surface. The non-integer peaks due to the ZnPc reconstruction are indicated by the dark yellow-shaded area, for the clearness of the figure background is not reported. The red thick line is the best fit to the data. (B) A possible model of growth of the monolayer of ZnPc on the Al(100) surface compatible with the 5 × 5 reconstruction deduced from the diffraction pattern. (C) Kinematics of the diffraction experiment, electron source, and analyzer are fixed, their directions form an angle of $2\theta_o$ equal to 30°. The variation in the $\Delta k_{\parallel}$ is obtained by means of a rotation of the sample (aa') described by the angle θ.

microscopy (STM) tip, which is able to remove the two hydrogen atoms and replace them with a silver atom, taken from the substrate.[16] A monolayer of H_2Pc grown on Ag(110) can spontaneously substitute the two hydrogen atoms with a silver atom.[17] In this case, the rate of the self-metalation process increases by heating the sample.[17] This suggests that it is possible not only to modify the molecule by means of the interaction with the substrate but also to control the rate at which the process occurs by controlling the substrate temperature. Another interesting process involving the central metal atom is the on-surface metalation of air-unstable Pc occurring for instance in the case of the synthesis of magnetic AlPc on the Au(111) surface.[18]

The reverse process, demetalation, consists in the extraction of the central metal atom from a MPc. It has been observed in the PbPc/Ag(111) interface where, with the aid of a STM tip, the Pb atom was extracted from the center of the molecule.[19] In this particular case, the spill out of the central atom is favored by the injection of electrons in the empty states of the molecule. The consequences on the morphological and electronic properties of the ligand are crucial aspects to be considered in the metalation and demetalation (whether spontaneous or stimulated) processes. To this end, spectroscopy such as UV−vis has been employed to test the integrity of the ligand after the demetalation of the molecule.[20] A valid alternative can be the X-ray photoemission spectroscopy (XPS) with its atomic and chemical-state sensitivities.

Up to now, the spontaneous loss of the central metal atom of a phthalocyanine interacting with a surface has never been observed. In this work, we present the first evidence of such a process occurring at the ZnPc/Al(100) interface. The self-demetalation presented and discussed here is the result of a particular combination of the strong interaction of the molecule with the substrate, the electronic structure of the molecule, and the binding energy of the Zn atom. The strong interaction of metal-Pc with the Al(100) surface was already observed in the case of CuPc.[13] In this case, a charge transfer from the metal substrate toward the molecular LUMO is observed. It is important to note here that, in the case of controlled demetalation in PbPc/Ag(110) interface, the charge transfer induced by the polarization of the STM tip seems to play a fundamental role. In the case of CuPc, any self-demetalation on the Al(100) surface was not observed. An important difference between CuPc and ZnPc is the binding energy of the metal atom with the macrocycle, lower in the latter case.[9] This energy difference will be taken into account while discussing the results presented in this work.

Furthermore, it is interesting to study the interface ZnPc/Al(100) because of its technological applications. Among others, the ZnPc/Al(100) interface is used in solar cells[21,22] where the phthalocyanine film is the absorber layer and the cathode is made of aluminum. From the point of view of electronic devices, it is well known that long-range-ordered systems improve the conductivity of organic semiconductors:[23] thick layers of Pcs form characteristic crystal structures driven also by the substrate and interaction of the substrate with the first Pc layer.[24] Previous works on CuPc/Al(100) interface does not show any ordered Pc overlayer. The molecular mobility is in fact reduced due to the strong interaction occurring at the interface. Ordered depositions of different Pcs

https://dx.doi.org/10.1021/acs.jpcc.0c06980
J. Phys. Chem. C 2020, 124, 22550−22558

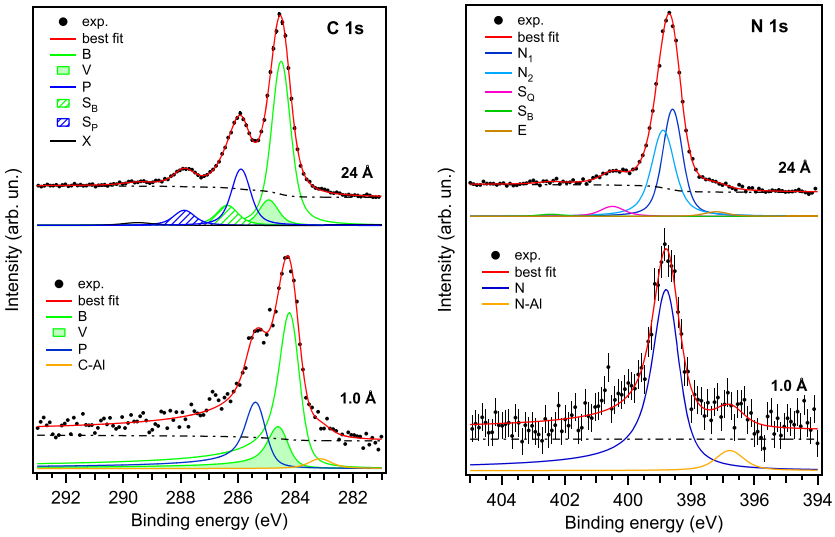

Figure 2. Best fit of the C 1s level (left) and N 1s (right) in bulk (top) and the submonolayer phase (bottom) grown with the substrate at T_s = RT. The best fitting parameters are reported in Table 1. The two spectra are normalized to show the differences between the two line shapes.

were, on the contrary, found on several systems, for instance, CuPc on Au(110) with molecules disposed as chains,[25] as square lattices on InAs and InSb(100)[26] and CoPc on Ag-terminated Si(111) as a close-packed array.[27] In addition, a 5 x 5 reconstruction is obtained in the event that metal Pcs are grown on the fcc(100) single-crystal.[28−32] In this paper, we investigate the possibility to grow an ordered ZnPc layer and increase the molecular mobility on the surface by thermally annealing the Al substrate during the Pc deposition. Finally, we studied different coverages of ZnPc to obtain information on the molecular structure at the interface by comparing the submonolayer and bulk phases.

MATERIALS AND METHODS

The Al(100) single-crystal was cleaned by several cycles of Ar^+ sputtering (2 keV) and annealing at 500 °C. At the end of the cleaning procedure, no oxygen and carbon contamination was detected by means of XPS and a sharp pattern was observed in electron diffraction measurements. ZnPc molecules, purity 95%, have been purchased from Sigma-Aldrich. Prior to any deposition on the Al sample, the molecules were further purified in ultrahigh-vacuum (UHV) for 5 h at 200 °C well below the sublimation temperature. ZnPc films on Al(100) were grown with a nominal evaporation rate of 0.2 Å/min on the substrate, kept at temperature T_s. Film thickness was deduced from the ratio of XPS signals of the C 1s from the overlayer and Al 2s from the substrate.[33] Films of different thicknesses (1 Å < θ < 24 Å) and grown at different substrate temperatures between room temperature (RT) and 160 °C are analyzed and discussed in this work. All the XPS spectra and diffraction patterns were acquired at RT. The photoemission spectra and electron diffraction patterns were acquired by means of an hemispherical analyzer (66 mm mean radius) equipped with a multichannel detector for parallel energy acquisition. For XPS measurements, a monochromatized Al Kα source provided photons with energy $h\nu$ = 1486.7 eV. The total experimental uncertainty in XPS spectra is equal to 0.56 eV. Absolute energy calibration was obtained by comparing the measured binding energy of the Al 2s peak with the value found in literature (E_b = 118.0 eV).[34] Diffraction experiments were conducted using a home-built monochromatic electron gun with a primary energy of E_p = 51.4 eV and an energy resolution of 60 meV. The uncertainty of the diffraction patterns is given by the angular resolution of the electron beam equal to ±0.5°. Since the electron source and analyzer are fixed, electron diffraction patterns were obtained by rotating the sample around the axis orthogonal to the scattering plane and are illustrated in Figure 1.

In our regression analysis of XPS spectra, we used Voigt's profile to fit symmetric peaks and Doniach−Sunjic's function convoluted with Gaussian for asymmetric ones. We used also a Shirley background, which is proportional to the integral of the fitted peaks. Background's parameters are free parameters of our regression analysis. In our analysis, we used the constrain that the Gaussian full width at half maximum (FWHM) of peaks must be equal or greater than the experimental uncertainty.

RESULTS AND DISCUSSION

Morphology of ZnPc Submonolayer Film. Figure 1 shows the evolution of the diffraction pattern along the $\bar{\Gamma}\bar{X}$ direction of different ZnPc films of the same thickness (1 Å) deposited on Al(100) and grown as a function of the substrate temperature (T_s). The patterns were obtained by measuring the sample at room temperature and after aligning the [10] surface direction of the sample with the scattering plane; to vary the projection of the exchanged wave vector on the sample surface ($\Delta k_{\parallel}$), the sample was rotated around an axis orthogonal to that plane. The shaded peaks are assigned to the specular peak ($\Delta k_{\parallel}$ = 0) and the (1,0) and ($\bar{1}$,0) Bragg peaks of the substrate. The average of the two Bragg peaks is $\Delta k_{\parallel}$ = 2.18 ± 0.02 $Å^{-1}$ corresponding to a distance between aluminum atoms of d_{Al} = 2.88 ± 0.03 Å, in very good agreement with the expected value of 2.86 Å.[35]

The deposition of 1 Å of ZnPc leads to the appearance of non-integer Bragg peaks with a 5-fold-decreased distance. Analogous diffraction pattern is observed when the azimuth is rotated by 90° and the [01] direction is aligned along the scattering plane. This indicates that ZnPc molecules give rise to a (5 × 5) reconstruction on Al(100), forming ordered domains with a square unit cell. Given this five-fold reconstruction, the molecule−molecule distance d_{ZnPc} is

https://dx.doi.org/10.1021/acs.jpcc.0c06980
J. Phys. Chem. C 2020, 124, 22550−22558

Table 1. Best Value of Fit Parameters of Bulk (24 Å) and Submonolayer Phase (1 Å) of C 1s Level (Upper Part) and N 1s Level (Lower Part) Grown with the Substrate at T_s = RT[a]

C 1s						
θ (Å)	peak	α	A	BE (eV)	GW (eV)	LW (eV)
24	B		1	284.48 ± 0.01	0.56 ± 0.01	0.38 ± 0.01
	V		0.16 ± 0.03	284.91 ± 0.03		
	P		0.34 ± 0.02	285.88 ± 0.01		
	S_B		0.14 ± 0.02	286.355 ± 0.03		0.52 ± 0.03
	S_P		0.11 ± 0.01	287.85 ± 0.01		
	X		0.03 ± 0.01	289.48 ± 0.05		1.0 ± 0.2
1	B	0.17 ± 0.01	1	284.14 ± 0.01	0.60 ± 0.02	0.28 ± 0.03
	V		0.27 ± 0.08	284.54 ± 0.07		
	P		0.43 ± 0.02	285.33 ± 0.015		
	C-Al	0	0.06 ± 0.02	283.1 ± 0.1	0.6 ± 0.3	0.6 ± 0.3
N 1s						
θ (Å)	peak	α	A	BE (eV)	GW(eV)	LW (eV)
24	N_1		1	398.60 ± 0.04	0.58 ± 0.01	0.28 ± 0.1
	N_2		1	398.88 ± 0.04		0.49 ± 0.06
	S_Q		0.12 ± 0.04	400.50 ± 0.05		0.51 ± 0.2
	S_B		0.027 ± 0.025	402.44 ± 0.20		0.6 ± 0.9
	E		0.05 ± 0.02	397.2 ± 0.1	0.59	0.49
1	N	0.11 ± 0.02	1	398.75 ± 0.01	0.56 ± 0.09	0.58 ± 0.09
	N-Al	0	0.095 ± 0.03	396.78 ± 0.02	0.7 ± 0.3	

[a]Fit displayed in Figure 2. θ is the overlayer thickness, α represents the asymmetry parameter of Doniach−Sunjic's function, A is the peak area normalized to the greatest one, BE is the binding energy, GW is the full Gaussian width at half maximum, and LW is the full Lorentzian width at half maximum.

equal to 5 × d_{Al} = 14.4 ± 0.15 Å. This distance is large enough to accommodate ZnPc in a flat lying geometry. In Figure 1, the diffraction pattern of a CuPc film grown with T_s = 160 °C is also reported. We observe a diffraction pattern very similar to the ZnPc case, indicating that the increased mobility occurring at this substrate temperature is efficient also in the case of CuPc. This adsorption geometry was already observed in other MPc/metal interfaces. In particular, CuPc, FePc, CoPc, and NiPc grown on Ag(100)[31] give rise to a flat lying geometry and azimuthal rotation of the phthalocyanine symmetry axis (dashed line in Figure 1B) of 30° with respect to the [10] direction. Analogous behavior is observed in the CoPc/Cu(100) interface.[32] Considering that Ag and Cu substrates have the same crystal structures (fcc) and orientation (100) of Al and that the interatomic distance is similar for Ag (2.89 Å) and even smaller for Cu (2.54 Å), we can safely guess that, also in the case of the Al substrate, the growth of Pc in the very early stage follows a flat lying geometry with a possible azimuthal rotation of the Pc symmetry axis.

A careful analysis reveals that the diffraction pattern becomes sharper at higher substrate temperature during the growth. As judged from the width of the non-integer Bragg peaks,[36] the size of the ordered ZnPc domains increases by a factor of 2 (from 40 to 80 Å) when T_s is raised from RT to 160 °C.

Electronic Structure of the ZnPc/Al Interface. To study the electronic structure at the interface between ZnPc and Al(100), a comparison between the line shapes of photoemission peaks in the submonolayer and bulk phase grown with the substrate at T_s = RT is reported. On top of Figure 2, we see respectively the characteristic spectra of C 1s and N 1s of Pc in the bulk phase. In the C 1s spectrum, there are three main peaks. As was done in other works,[13,37] they are deconvoluted using five symmetric components, whose parameters are reported in Table 1.

The five components represent carbon atoms in the benzene ring (B) and the associated shake-up satellite (S_B), carbon atoms in the pyrrolic ring (P) and the associated shake-up (S_P), finally V is the vibrational C−H stretching mode. It is well known that the two shake-ups S_P and S_B are electron excitations involving the HOMO−LUMO transition (1.9 eV[37]). A possible quality factor of the fit is the evaluation of the stoichiometric ratio of inequivalent carbon atoms. The ratio of signals coming from benzene carbon (B, V, S_B) and pyrrolic carbon (P and S_P) is equal to 2.9 ± 0.2 in agreement, within the experimental uncertainty, with the expected stoichiometric ratio (3). To reproduce the experimental signal, a sixth component called X is close to 289 eV. It should correspond to unresolved shake-ups of higher energy, related to the electronic transition localized on both benzenic and pyrrolic carbons.[38]

The spectrum of the bulk phase N 1s level is reported in the upper part of Figure 2; it is possible to observe one main peak with two much smaller peaks on its sides. Our best fit of bulk phase's, reported on top of Figure 2, is not different from other phthalocyanine bulk phases;[37,39] all components are symmetric and their parameters are reported in Table 1. The components are attributed to nitrogen in the pyrrolic ring (N_1), nitrogen in aza-bridging positions (N_2), two shake-ups satellites (S_Q and S_B) that correspond to[37,39] Q band (HOMO−LUMO transition) and B band ($a_{2u} \rightarrow e_g$, $b_{1g} \rightarrow e_g$, and $e_u \rightarrow e_g$).[40] The component E is attributed to a contamination whose origin is not clear. Its intensity is only 2.3 ± 0.1% of the total nitrogen signal, small enough not to hinder the analysis of the

https://dx.doi.org/10.1021/acs.jpcc.0c06980
J. Phys. Chem. C 2020, 124, 22550−22558

Table 2. Best Value of Fit Parameters of Sub-monolayer 1 Å and Bulk Phase 24 Å of Zn $2p_{3/2}$ Level Grown with the Substrate at T_s = RT[a]

θ (Å)	α	A (A.U.)	BE (eV)	GW (eV)	LW (eV)
24		16.96 ± 0.07	1021.97 ± 0.01	0.56 ± 0.02	0.95 ± 0.01
1	0.10 ± 0.01	2.07 ± 0.24	1021.36 ± 0.01	0.56 ± 0.06	0.73 ± 0.05

[a]Fit displayed in Figure 3. θ is the overlayer thickness, α represents the asymmetry parameter of Doniach−Sunjic function, A is the peak area, BE is the binding energy, GW is the full Gaussian width at half maximum, and LW is the full Lorentzian width at half maximum.

signal of the molecule. Moreover, we impose the areas of N_1 and N_2 to be equal in our fit because, as can be seen in Figure 1, there are four nitrogen atoms in the pyrrolic ring, which are bond to the metal and carbon, and four in aza-bridging positions, bond only to carbon.

C 1s and N 1s spectra in the submonolayer phase, lower part of Figure 2, are quite different from the corresponding spectra in the bulk phase. On the contrary, they show strong similarities with the respective spectra of the submonolayer phase in the CuPc/Al(100) interface.[13] In particular, we observe the following: the quenching of shake-ups, the asymmetric shape for C 1s and N 1s peaks, attributed to the hybridization of LUMO with Al bands,[13] and a shift of the C 1s level, originating from a charge transfer from aluminum to LUMO.[13] In both submonolayer spectra, we found also two components at lower binding energy; they can be attributed to a small amount of carbon (C-Al) and nitrogen (N-Al) atoms interacting with aluminum,[41] stemming from C/N contamination during Al surface preparation. From the analysis of the C 1s submonolayer spectrum, we obtain, see Table 1, that the ratio between the sum of B and V divided by P is equal to 2.9 ± 0.2, in agreement with the expected stoichiometric ratio of molecular constituents equal to 3. From the same table, we observe that the C 1s binding energy shift of pyrrolic carbon between bulk and the submonolayer is equal to 0.55 ± 0.02 eV, while the energy shift of benzene carbon is equal to 0.34 ± 0.02 eV. This difference can be explained considering that the aforementioned charge transfer from the substrate toward the LUMO is not uniform on the whole molecule but it is more pronounced where the LUMO is localized. Considering the spatial distribution of the LUMO, mainly localized on the pyrrolic ring,[42,43] we expect a greater charge transfer on pyrrolic carbon with respect to the benzenic carbon hence a greater shift of the corresponding binding energy. In principle, the LUMO is also localized on N bonded to pyrrolic carbon but, as discussed later on, that atom seems to be not involved in the charge transfer. The main peak of the N 1s spectrum is deconvoluted with a single component (N); in this case, N represents both the nitrogen atoms in pyrrolic and the aza-bridging positions. If we consider its binding energy (398.75 eV) as the mean binding energy of the two inequivalent nitrogen atoms and compare it with the mean of the two distinct components in the bulk phase, we observe almost no shift between them. A hypothesis to explain this is consistent with the calculations on the isolated molecule[9] where we observe that nitrogen atoms are slightly negatively charged, while carbon atoms are positive; then the charge transfer occuring at the interface involves mostly carbon atoms and not nitrogen atoms.[13]

In Figure 3, we report the evolution of Zn $2p_{3/2}$ as a function of coverage; the corresponding thickness is reported on the right side of each spectrum, top and bottom spectra are, respectively, the bulk and submonolayer phases. Bulk and submonolayer phases are both deconvoluted with one peak,

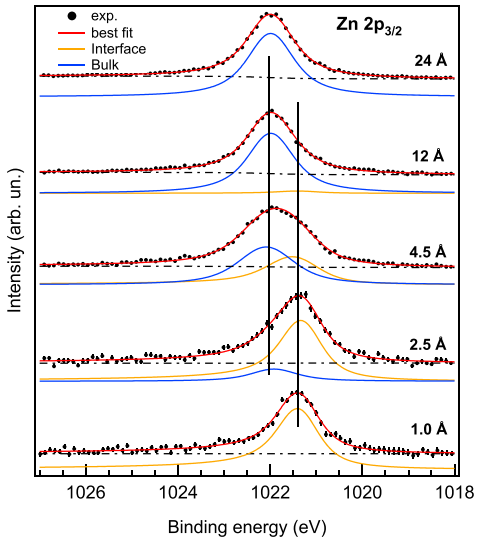

Figure 3. Zn $2p_{3/2}$ XPS spectra as a function of ZnPc coverage. The samples were grown with the substrate at T_s = RT. Zn atoms in different oxidation states, Zn(0) at the interface and Zn(II) in the bulk, are represented by orange and blue lines, respectively. The best fitting parameters are reported in Table 2. The spectra are normalized to show the evolution of the line shapes as a function of the coverage.

symmetric in the former case and asymmetric in the latter. The binding energies of the two peaks are shifted by about 600 meV. Fitting parameters are reported in Table 2. The intermediate coverage spectra are deconvoluted with two components whose binding energy corresponds to the binding energy of the single components observed in the thick and monolayer cases. In previous discussion on the analysis of N 1s and C 1s spectra in the submonolayer phase, we attributed the peak asymmetry and bulk to submonolayer binding energy shift to the charge transfer from the substrate to the LUMO and to its hybridization with Al bands. This explanation cannot be extended to a shift of 600 meV in Zn $2p_{3/2}$ because we do not expect any charge transfer to the Zn atom. In fact, the LUMO is not localized on zinc and the b_{1g} orbital (involved in the charge transfer in CuPc/Al(100) interface)[13] is initially occupied. The observed binding energy shift of 600 meV in zinc spectra is equal to the energy difference between divalent (Zn(II)), configuration of zinc in isolated Pc, and metallic (Zn(0)) zinc.[44,45] Moreover, the Lorentzian widths of bulk and submonolayer phases are significantly different (0.95 and 0.73 eV) and they are in agreement with the ones measured for ZnO (Zn(II)) and metallic zinc (Zn(0)),[44] respectively. All these results clearly indicate that in the submonolayer phase, Zn is in metallic configuration. This configuration is possible only if Zn forms a metal cluster or Zn−Al metal alloy. These hypotheses are discussed in the next section.

Demetalation and Diffusion of Zn Atoms. In this section, the photoemission spectra of Zn $2p_{3/2}$, C 1s, and N 1s

https://dx.doi.org/10.1021/acs.jpcc.0c06980
J. Phys. Chem. C 2020, 124, 22550−22558

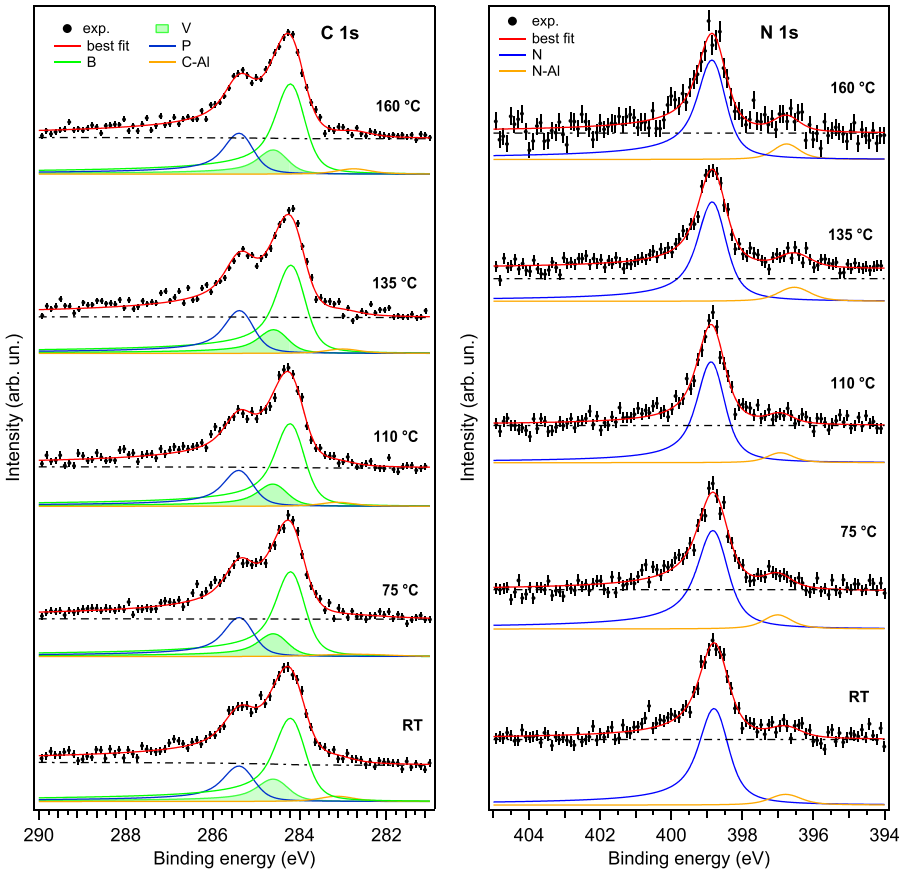

Figure 4. C 1s and N 1s XPS spectra of ZnPc submonolayer films (θ = 1 Å) as a function of the substrate temperature T_s at which the sample was kept during the growth. All the spectra are collected at RT.

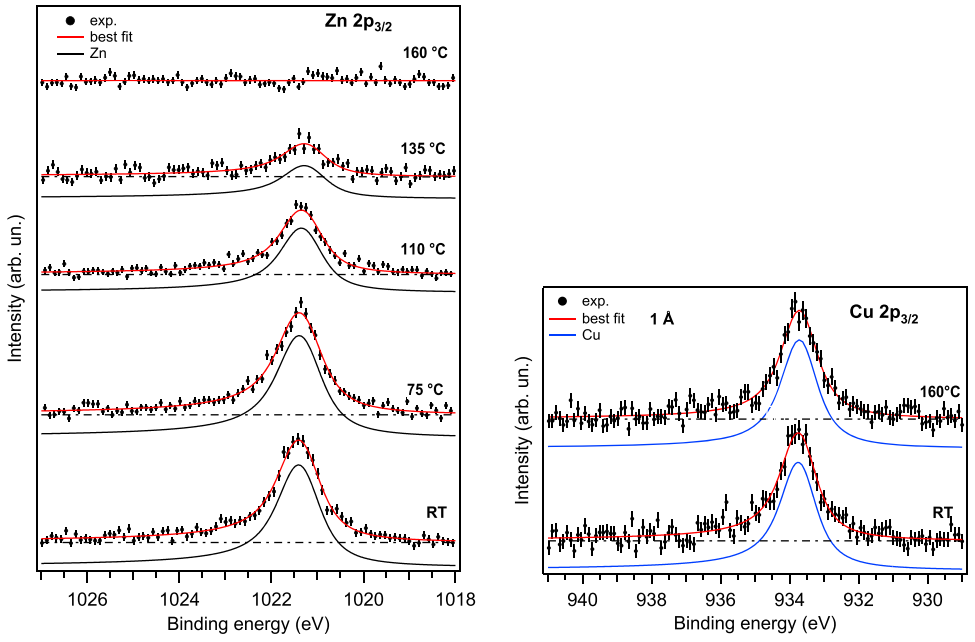

Figure 5. Zn $2p_{3/2}$ (left) and Cu $2p_{3/2}$ (right) XPS spectra of ZnPc and CuPc, submonolayer films (θ = 1 Å) as a function of the substrate temperature T_s during the growth. All the spectra are collected at RT.

core levels as a function of substrate temperature during the growth of ZnPc will be presented and discussed. For each substrate temperature (T_s), a new film of about 1 Å of thickness was prepared. The spectra of C 1s and N 1s are presented in Figure 4. No significant variation in the photoemission spectra is observed with respect to the spectra where ZnPc is grown at RT. In particular, the spectra of C 1s and N 1s were deconvoluted with the same line shape discussed previously (see section Electronic Structure of the ZnPc/Al Interface) suggesting that the electronic structure of

https://dx.doi.org/10.1021/acs.jpcc.0c06980
J. Phys. Chem. C 2020, 124, 22550−22558

the ligand at the interface is independent of the substrate temperature during the growth. Moreover, spectra of C 1s and N 1s in the ZnPc/Al(100) interface are very similar to the corresponding spectra of the CuPc/Al(100) interface,[13] suggesting that the Pc ring is intact for all T_s's. In Figure 5, the Zn $2p_{3/2}$ spectra are reported as a function of T_s; we observe a progressive reduction of photoemission signal starting from T_s = 110 °C; at T_s = 160 °C, the photoemission signal from Zn $2p_{3/2}$ completely disappears. For T_s = 160 °C, the ligand is intact while the vanishing of the Zn 2p photoemission signal can be explained with the loss of the Zn atom from the center of the molecule and its diffusion inside the Al substrate. Diffusion of zinc in aluminum is a well-known phenomenon facilitated by the increase of the substrate temperature.[46] On the contrary, the influence of the substrate temperature on the loss of Zn atoms from the center of the molecule is less clear. To answer this key question, it is useful to note the results of photoemission signal of Zn when the film is grown with the sample taken at RT; in that case, we observed an asymmetric line shape and core level shift compatible with Zn in metallic configuration. Moreover, the absence of any energy shift or change in line shapes of C 1s and N 1s as a function of T_s supports the idea that the macrocycle has the same electronic configuration for all T_s. All these experimental results suggest that the Zn atom leaves the center of the molecule also if ZnPc film is grown at RT. In this case, the metallic configuration of Zn atoms can be ascribed to the formation of the Zn metal cluster or to Al−Zn alloy. Only when T_s is greater than a threshold value (between 75 and 110 °C), Zn starts to diffuse in the bulk of the substrate. The behavior of ZnPc is different from that of CuPc growth on the same Al(100) substrate. In fact, as shown in the right part of Figure 5, the CuPc film grown with the same T_s does not show any loss of the central metal atom. Moreover, as previously observed,[13] the line shape of Cu 2p is symmetric after the growth either at RT or at T_s = 160 °C. To explain the difference between ZnPc and CuPc, we have to consider that the thermal stability of the molecule is not questioned because the maximum substrate temperature during the deposition is well below the sublimation temperature and the results from the thick film of ZnPc confirms the entirety of the molecule after sublimation. Binding energy of the central metal atom to the ligand[9] can play a role in the loss of the Zn atom from the center of Pc because the calculated M−Pc binding energy for the Zn atom is lower with respect to the Cu atom in CuPc and it is the lowest among the M−Pc's calculated in ref 9. Nevertheless, the break of the metal−ligand bond is clearly related to the substrate because the loss of Zn has been observed only in this particular case of the submonolayer film grown on Al(100). Recently, the demetalation of the phthalocyanine at the PbPc/Ag(110) interface[19] was reported. In that case, the process is driven by a strong polarization of the STM tip with respect to the substrate. The induced demetalation by the STM tip is not effective when a low bias is applied. Then, the polarization causes the injection of charges in the empty states of the phthalocyanine and this can induce the loss of the central metal atom.[19] Analogous mechanism can occur also in our case where the charge transfer from the substrate to the LUMO is a consequence of the interface formation as discussed previously (see section Electronic Structure of the ZnPc/Al Interface); hence, the demetalation can be a direct consequence of the charge transfer occuring at the ZnPc/Al(100) interface. The same effect is not observed in the case of CuPc/Al(100) interface. As previously mentioned, the binding energy of Zn atom in ZnPc is lower with respect to the Cu binding energy in CuPc; moreover, the empty molecular states in the two molecules (ZnPc and CuPc) for the charge transfer from the substrate are slightly different. While the LUMO, with the original e_g symmetry, is practically the same in the two molecules, in the case of CuPc also, b_{1g} is involved in the charge transfer.[13] This involvement redirects part of the charge toward the copper atom and then modifies the charge transfer toward the ligand. The different charge transfer could be the origin of the demetalation observed only for the ZnPc/Al interface. The last topic that we would discuss concerns the evolution of the structure of the ligand after the loss of the Zn atom. Is the central atom replaced? In principle, Zn atoms can be substituted by two H atoms; we do not observe the fingerprint of this process, i.e., a component in the N 1s core level spectrum shifted of 1.4 eV with respect to the bridging component.[47] Another possibility is that the Zn atom is substituted by an Al atom coming from the substrate. From the spectroscopic point of view, this hypothesis is compatible with our results because the N 1s spectrum is not substantially modified when the Al atom is in the center of the molecule as observed in the case of vacuum synthesis of AlPc[18] and the difference in Al spectrum is not detectable due to the very low density of Al atoms eventually bonded in the center of the molecule. Further investigations are needed to clarify this point.

CONCLUSIONS

The comparison of submonolayer and bulk phase spectra of C 1s and N 1s suggests a strong interaction of ZnPc with the Al(100) substrate. In particular, the modification of the line shape of C 1s and N 1s core levels, i.e., the inhibition of the HOMO−LUMO transition, the asymmetry of the photoemission peak shape, in the afore mentioned photoemission peaks, and their relative energy shifts, can be explained with the hybridization of LUMO with Al(100) bands and a charge transfer from the substrate to the LUMO. From this point of view, this interface is very similar to the CuPc/Al(100) interface.[13] Also, the morphology of the two interfaces is similar; in fact, in both cases, the long range order associated with the 5 × 5 reconstruction improves when higher substrate temperatures are set-up during the growth. The maximum extension of ordered domains reaches 80 Å at T_s = 160 °C.

The peculiarity of the present study on the ZnPc/Al interface is the observation of the self-demetalation of the phthalocyanine. The loss of the central metal atom already during the growth at RT is promoted by the charge transfer occuring at the ZnPc/Al interface. The loss of Zn atoms is deduced from the asymmetric line shape of the Zn 2p core level and from its energy shift with respect to the energy position in thick ZnPc films. Increasing the substrate temperature up to T_s = 160 °C supports the diffusion of Zn atoms in the Al substrate. The loss of the central metal atom does not modify significantly the electronic structure of the ligand at all studied growth temperatures between RT and T_s = 160 °C as deduced from the C 1s and N 1s core level spectra.

AUTHOR INFORMATION

Corresponding Author

Alessandro Ruocco − *Dipartimento di Scienze, Università degli Studi Roma Tre, Rome 00146, Italy;* orcid.org/0000-0002-

https://dx.doi.org/10.1021/acs.jpcc.0c06980
J. Phys. Chem. C 2020, 124, 22550−22558

4909-7216; Phone: +390657337210;
Email: alessandro.ruocco@uniroma3.it

Authors

Daniele Paoloni − *Dipartimento di Scienze, Università degli Studi Roma Tre, Rome 00146, Italy*

Gianluca Di Filippo − *Dipartimento di Scienze, Università degli Studi Roma Tre, Rome 00146, Italy*

Dean Cvetko − *University Ljubljana, Faculty for mathematic and physics, Ljubljana SI-1000, Slovenia; Institute J. Stefan, Ljubljana SI-1000, Slovenia; Laboratorio TASC CNR-IOM, Trieste 34127, Italy*

Gregor Kladnik − *University Ljubljana, Faculty for mathematic and physics, Ljubljana SI-1000, Slovenia; Laboratorio TASC CNR-IOM, Trieste 34127, Italy;* orcid.org/0000-0002-8675-4756

Alberto Morgante − *Physics Department, University of Trieste, Trieste 34127, Italy; Laboratorio TASC CNR-IOM, Trieste 34127, Italy;* orcid.org/0000-0001-9021-2944

Complete contact information is available at:
https://pubs.acs.org/10.1021/acs.jpcc.0c06980

Notes

The authors declare no competing financial interest.

■ ACKNOWLEDGMENTS

Partial financial support by Università Roma Tre, "Piano Straordinario della Ricerca 2015, azione n. 3 -Potenziamento dei laboratori di ricerca-" is greatly acknowledged. D.C. and G.K. acknowledge partial financial support from the Slovenian Research Agency (P1-0112, and P1-0044). A.M. acknowledges support from the Ministero dell'Istruzione, dell'Università e della Ricerca (PRIN 2017KFY7XF_002). We are grateful to Guido Fratesi for his critical reading of the manuscript.

■ REFERENCES

(1) Edwards, L.; Gouterman, M. Porphyrins: XV. Vapor absorption spectra and stability: Phthalocyanines. *J. Mol. Spectrosc.* **1970**, *33*, 292−310.

(2) Tataroğlu, A.; Tuncer, H.; Al-Ghamdi, A. A.; Dere, A.; Arif, B.; Yol, S.; Ozdemir, N.; El-Tantawy, F.; Yakuphanoglu, F. Graphene−cobalt phthalocyanine based on optoelectronic device for solar panel tracking systems. *Synth. Met.* **2015**, *206*, 15−23.

(3) Miasik, J. J.; Hooper, A.; Tofield, B. C. Conducting polymer gas sensors. *J. Chem. Soc., Faraday Trans. 1* **1986**, *82*, 1117−1126.

(4) Tongpool, R.; Yoriya, S. Kinetics of nitrogen dioxide exposure in lead phthalocyanine sensors. *Thin Solid Films* **2005**, *477*, 148−152.

(5) Wen, Z.-H.; Kang, T.-F. Determination of nitrite using sensors based on nickel phthalocyanine polymer modified electrodes. *Talanta* **2004**, *62*, 351−355.

(6) Blochwitz, J.; Pfeiffer, M.; Fritz, T.; Leo, K. Low voltage organic light emitting diodes featuring doped phthalocyanine as hole transport material. *Appl. Phys. Lett.* **1998**, *73*, 729−731.

(7) Bruder, I.; Ojala, A.; Lennartz, C.; Sundarraj, S.; Schöneboom, J.; Sens, R.; Hwang, J.; Erk, P.; Weis, J. Theoretical and experimental investigation on the influence of the molecular polarizability of novel zinc phthalocyanine derivatives on the open circuit voltage of organic hetero-junction solar cells. *Sol. Energy Mater. Sol. Cells* **2010**, *94*, 310−316.

(8) Terao, Y.; Sasabe, H.; Adachi, C. Correlation of hole mobility, exciton diffusion length, and solar cell characteristics in phthalocyanine/fullerene organic solar cells. *Appl. Phys. Lett.* **2007**, *90*, 103515.

(9) Liao, M.-S.; Scheiner, S. Electronic structure and bonding in metal phthalocyanines, Metal=Fe, Co, Ni, Cu, Zn, Mg. *J. Chem. Phys.* **2001**, *114*, 9780−9791.

(10) Lever, A. B. P. *Advances in Inorganic Chemistry and Radiochemistry*; Emeléus, H. J.; Sharpe, A. G., Eds.; Academic Press: New York, 1965; Vol. 7; pp. 27−114.

(11) Isvoranu, C.; Wang, B.; Schulte, K.; Ataman, E.; Knudsen, J.; Andersen, J. N.; Bocquet, M. L.; Schnadt, J. Tuning the spin state of iron phthalocyanine by ligand adsorption. *J. Phys.: Condens. Matter* **2010**, *22*, 472002.

(12) Wang, Y.; Kröger, J.; Berndt, R.; Hofer, W. A. Pushing and Pulling a Sn Ion through an Adsorbed Phthalocyanine Molecule. *J. Am. Chem. Soc.* **2009**, *131*, 3639−3643.

(13) Ruocco, A.; Evangelista, F.; Gotter, R.; Attili, A.; Stefani, G. Evidence of Charge Transfer at the Cu-phthalocyanine/Al(100) Interface. *J. Phys. Chem. C* **2008**, *112*, 2016−2025.

(14) Song, C.-L.; Wang, Y.-L.; Ning, Y.-X.; Jia, J.-F.; Chen, X.; Sun, B.; Zhang, P.; Xue, Q.-K.; Ma, X. Tailoring Phthalocyanine Metalation Reaction by Quantum Size Effect. *J. Am. Chem. Soc.* **2010**, *132*, 1456−1457.

(15) Bai, Y.; Buchner, F.; Wendahl, M. T.; Kellner, I.; Bayer, A.; Steinrück, H.-P.; Marbach, H.; Gottfried, J. M. Direct Metalation of a Phthalocyanine Monolayer on Ag(111) with Coadsorbed Iron Atoms. *J. Phys. Chem. C* **2008**, *112*, 6087−6092.

(16) Sperl, A.; Kröger, J.; Berndt, R. Controlled Metalation of a Single Adsorbed Phthalocyanine. *Angew. Chem.* **2011**, *50*, 5294−5297.

(17) Smykalla, L.; Shukrynau, P.; Zahn, D. R. T.; Hietschold, M. Self-Metalation of Phthalocyanine Molecules with Silver Surface Atoms by Adsorption on Ag(110). *J. Phys. Chem. C* **2015**, *119*, 17228−17234.

(18) Hong, I.-P.; Li, N.; Zhang, Y.-J.; Wang, H.; Song, H.-J.; Bai, M.-L.; Zhou, X.; Li, J.-L.; Gu, G.-C.; Zhang, X.; et al. Vacuum synthesis of magnetic aluminum phthalocyanine on Au(111). *Chem. Commun.* **2016**, *52*, 10338−10341.

(19) Sperl, A.; Kröger, J.; Berndt, R. Demetalation of a Single Organometallic Complex. *J. Am. Chem. Soc.* **2011**, *133*, 11007−11009.

(20) Prado, G. H. C.; de Klerk, A. Demetalation of metallophthalocyanines by mild halogenation without disrupting the tetrapyrrole macrocycle. *Fuel* **2015**, *161*, 43−48.

(21) Singh, V. P.; Singh, R. S.; Parthasarathy, B.; Aguilera, A.; Anthony, J.; Payne, M. Copper-phthalocyanine-based organic solar cells with high open-circuit voltage. *Appl. Phys. Lett.* **2005**, *86*, No. 082106.

(22) Loutfy, R. O.; Sharp, J. H. Photovoltaic properties of metal-free phthalocyanines. I. Al/H2Pc Schottky barrier solar cells. *J. Chem. Phys.* **1979**, *71*, 1211−1217.

(23) Dimitrakopoulos, C. D.; Mascaro, D. J. Organic thin-film transistors: A review of recent advances. *IBM J. Res. Dev.* **2001**, *45*, 11−27.

(24) Pierantozzi, G. M.; Sbroscia, M.; Ruocco, A. Templating effect of the substrate on the structure of Cu-phthalocyanine thin film. *Surf. Sci.* **2018**, *669*, 176−182.

(25) Floreano, L.; Cossaro, A.; Gotter, R.; Verdini, A.; Bavdek, G.; Evangelista, F.; Ruocco, A.; Morgante, A.; Cvetko, D. Periodic Arrays of Cu-Phthalocyanine Chains on Au(110). *J.Phys. Chem. C* **2008**, *112*, 10794−10802.

(26) Cox, J. J.; Bayliss, S. M.; Jones, T. S. Ordered copper phthalocyanine overlayers on InAs and InSb (100) surfaces. *Surf. Sci.* **1999**, *433-435*, 152−156.

(27) Upward, M. D.; Beton, P. H.; Moriarty, P. Adsorption of cobalt phthalocyanine on Ag terminated Si(111). *Surf. Sci.* **1999**, *441*, 21−25.

(28) Mugarza, A.; Lorente, N.; Ordejón, P.; Krull, C.; Stepanow, S.; Bocquet, M.-L.; Fraxedas, J.; Ceballos, G.; Gambardella, P. Orbital Specific Chirality and Homochiral Self-Assembly of Achiral Molecules Induced by Charge Transfer and Spontaneous Symmetry Breaking. *Phys. Rev. Lett.* **2010**, *105*, 115702.

(29) Colonna, S.; Mattioli, G.; Alippi, P.; Bonapasta, A. A.; Cricenti, A.; Filippone, F.; Gori, P.; Paoletti, A. M.; Pennesi, G.; Ronci, F.; et al. Supramolecular and Chiral Effects at the Titanyl Phthalocyanine/Ag(100) Hybrid Interface. *J. Phys. Chem. C* **2014**, *118*, 5255−5267.

(30) Salomon, E.; Beato-Medina, D.; Verdini, A.; Cossaro, A.; Cvetko, D.; Kladnik, G.; Floreano, L.; Angot, T. Correlation between Charge Transfer and Adsorption Site in CoPc Overlayers Adsorbed on Ag(100). *J. Phys. Chem. C* **2015**, *119*, 23422−23429.
(31) Mugarza, A.; Robles, R.; Krull, C.; Korytár, R.; Lorente, N.; Gambardella, P. Electronic and magnetic properties of molecule-metal interfaces: Transition-metal phthalocyanines adsorbed on Ag(100). *Phys. Rev. B* **2012**, *85*, 155437.
(32) Takada, M.; Tada, H. Direct observation of adsorption-induced electronic states by low-temperature scanning tunneling microscopy. *Ultramicroscopy* **2005**, *105*, 22−25.
(33) Fadley, C. S. *Electron Spectroscopy: Theory Techniques and Applications*; Brundle, C. R.; Baker, A. D., Eds.; Academic Press: London, 1978; Vol. 2; pp. 2−156.
(34) Ley, L.; McFeely, F. R.; Kowalczyk, S. P.; Jenkin, J. G.; Shirley, D. A. Many-body effects in x-ray photoemission from magnesium. *Phys. Rev. B* **1975**, *11*, 600−612.
(35) Davey, W. P. Precision Measurements of the Lattice Constants of Twelve Common Metals. *Phys. Rev.* **1925**, *25*, 753−761.
(36) Henzler, M. LEED studies of surface imperfections. *Appl. Surf. Sci.* **1982**, *11-12*, 450−469.
(37) Papageorgiou, N.; Ferro, Y.; Salomon, E.; Allouche, A.; Layet, J. M.; Giovanelli, L.; Le Lay, G. Geometry and electronic structure of lead phthalocyanine: Quantum calculations via density-functional theory and photoemission measurements. *Phys. Rev. B* **2003**, *68*, 235105.
(38) Salomon, E.; Papageorgiou, N.; Ferro, Y.; Layet, J. M. Electronic transitions and resonance electron scattering measured by electron energy loss spectroscopy of lead phthalocyanine thin film. *Thin Solid Films* **2004**, *466*, 259−264.
(39) Massimi, L.; Angelucci, M.; Gargiani, P.; Betti, M. G.; Montoro, S.; Mariani, C. Metal-phthalocyanine ordered layers on Au(110): Metal-dependent adsorption energy. *J.Chem. Phys.* **2014**, *140*, 244704.
(40) Nguyen, K. A.; Pachter, R. Ground state electronic structures and spectra of zinc complexes of porphyrin, tetraazaporphyrin, tetrabenzoporphyrin, and phthalocyanine: A density functional theory study. *J. Chem. Phys.* **2001**, *114*, 10757−10767.
(41) Molodtsova, O. V.; Aristova, I. M.; Babenkov, S. V.; Vilkov, O. V.; Aristov, V. Y. Morphology and properties of a hybrid organic-inorganic system: Al nanoparticles embedded into CuPc thin film. *J. Appl. Phys.* **2014**, *115*, 164310−164310.
(42) Evangelista, F.; Carravetta, V.; Stefani, G.; Jansik, B.; Alagia, M.; Stranges, S.; Ruocco, A. Electronic structure of copper phthalocyanine: An experimental and theoretical study of occupied and unoccupied levels. *J. Chem. Phys.* **2007**, *126*, 124709.
(43) Yanagisawa, S.; Yasuda, T.; Inagaki, K.; Morikawa, Y.; Manseki, K.; Yanagida, S. Intermolecular Interaction as the Origin of Red Shifts in Absorption Spectra of Zinc-Phthalocyanine from First-Principles. *J. Phys. Chem. A* **2013**, *117*, 11246−11253.
(44) Cabrera-German, D.; Molar-Velázquez, G.; Gómez-Sosa, G.; de la Cruz, W.; Herrera-Gomez, A. Detailed peak fitting analysis of the Zn 2p photoemission spectrum for metallic films and its initial oxidation stages. *Surf. Interface Anal.* **2017**, *49*, 1078−1087.
(45) Ballerini, G.; Ogle, K.; Barthés-Labrousse, M.-G. The acid-base properties of the surface of native zinc oxide layers: An XPS study of adsorption of 1,2-diaminoethane. *Appl. Surf. Sci.* **2007**, *253*, 6860−6867.
(46) Peterson, N. L.; Rothman, S. J. Impurity Diffusion in Aluminum. *Phys. Rev. B* **1970**, *1*, 3264−3273.
(47) Shariati, M.-N.; Lüder, J.; Bidermane, I.; Ahmadi, S.; Göthelid, E.; Palmgren, P.; Sanyal, B.; Eriksson, O.; Piancastelli, M. N.; Brena, B.; et al. Photoelectron and Absorption Spectroscopy Studies of Metal-Free Phthalocyanine on Au(111): Experiment and Theory. *J. Phys. Chem. C* **2013**, *117*, 7018−7025.

https://dx.doi.org/10.1021/acs.jpcc.0c06980
J. Phys. Chem. C 2020, 124, 22550−22558